Calculations of electron-impact single-ionization cross sections of helium isoelectronic systems

M. A. Uddin,[1] M. A. K. Fazlul Haque,[1] A. K. Basak,[1] and B. C. Saha[2]
[1]*Department of Physics, University of Rajshahi, Rajshahi-6205, Bangladesh*
[2]*Department of Physics, Florida A & M University, Tallahassee, Florida 32307, USA*
(Received 30 May 2004; published 16 September 2004)

The electron-impact single-ionization cross sections on the helium isoelectronic targets He, Li^{+}, B^{3+}, C^{4+}, N^{5+}, O^{5+}, Ne^{8+}, Na^{9+}, Fe^{24+}, Ag^{45+}, and U^{90+}, are calculated using the recent simplified version of the binary-encounter dipole (siBED) model as applied by Huo [Phys. Rev. A **64**, 042719 (2001)] to various molecular targets. The simple siBED model is good for the helium atom, but it is inadequate for ionic targets. Our proposed modifications: (i) ionic correction of the siBED model (QIBED) and (ii) relativistic corrections of the siBED model (RQIBED) are examined on a wider group of species and compared with other available experimental and theoretical results. The predictions of QIBED in the nonrelativistic energy domain and of RQIBED for all energies, with the same parameter values of siBED, produce excellent agreement with the experimental data and the results close to those of other theories for all the two-electron systems, neutral or ions on the same footing.

DOI: 10.1103/PhysRevA.70.032706 PACS number(s): 34.80.Dp

I. INTRODUCTION

The study of electron-impact ionization (EII) of atoms and ions is of fundamental importance for the basic understanding of collision physics and is useful for numerous applications in plasma kinetics problems, mass spectrometry, gas lasers, astrophysics, atmospheric physics, radiation science, and semiconductor physics. Because of the formidable experimental difficulties, the situation concerning the quantitative knowledge of the EII cross sections is still far beyond the need for many areas of application. The void in the experimental cross sections has to be filled in through generation of high-quality data by accurate theoretical methods. With the advent of fast computers, several quantal methods have been developed [1–11]. However, quantum calculations are arduous and become expensive even with the use of supercomputers. One can produce cross-section data just for some selected targets at some discrete energy points using the quantal theories just as are done with the experimental tools. Practical applications, however, require a quick estimation of a large number of reasonably accurate cross-section values often over a wider energy range and target species, which neither experiments nor rigorous methods generate easily. Thus simple to use semiempirical and semiclassical methods are commonly employed.

Reviews on the various theoretical studies on the electron impact ionization are provided in Refs. [12–14]. The most simple and widely used empirical formula for the calculations of EII cross sections was given by Lotz [15]. Bernshtam *et al.* [16] proposed a more accurate empirical formula (BRY) which they applied for ions of charge $q>1$. Gryzinski [17] proposed the ionization model in the frame work of classical binary-encounter approximation (BEA) assuming a continuous velocity distribution of the target electron. Vriens [18] modified the BEA with the inclusion of an exchange term and a term denoting the interference between the exchange and direct terms. Uddin *et al.* infused a relativistic factor in the Vriens' model to propose as the parameter-free RBEA model and to apply to the hydrogen [19] and helium [20] isoelectronic systems. Both the DM model (Deutsch and Märk [21]) and the binary-encounter dipole (BED) model of Kim and Rudd [22] have been widely applied to electron impact ionization of atoms and molecules. The BED model embodies a modified form of the Mott cross section and the Bethe-dipole cross section with the replacement of the incident electron energy $k_0^2/2$ by $(k_0^2+k_b^2+\alpha_0^2)/2$, where $k_b^2/2$ is the kinetic energy of the bound electron and $\alpha_0^2/2$ is its binding energy. The simplest version of the BED model is the binary-encounter Bethe (BEB) model [22]. The calculations based on either BED or BEB are generally in good agreement with the experimental data on simple atoms and molecules at incident energies from the threshold to several keV with the deviation within 5–15 % at the peak; the BED model, however, predicts better results than those of BEB model [23–27]. The relativistic extension of BEB is the RBEB model [28]. Although BED and BEB have demonstrated a considerable success particularly for molecular targets, there remains some puzzling aspects [29]. These models have been applied successfully at the threshold region, even though the high-energy Bethe approximation is employed. The replacement of the $k_0^2/2$ by $(k_0^2+k_b^2+\alpha_0^2)/2$ in the Bethe cross section also has no sound theoretical footing, albeit it works astonishingly well.

Huo [29] has recently modified the binary-encounter dipole (iBED) model by replacing the Bethe cross section at low energies with the dipole Born cross section. However, the two parameters in this model are species dependent and are related to the nature of the charge distribution in the bonding region. Nevertheless, Huo obtained a simplified version of the iBED (siBED) model, where the two parameters can assume a set of generic values [29]. These are applied with considerable success to the calculations of the EII cross sections of N_2, H_2O, CO_2, CH_4, and CF_4. To the best of our knowledge, neither iBED nor siBED has yet been applied to atomic systems. With respect to the incident electron the iBED predictions make no distinction between the collision with a neutral target and that with an ion. However, the differences, between the description of the target electron in neutrals and that in ions are accounted for through the kinetic energy $k_b^2/2$, the binding energy $\alpha_0^2/2$ of the target electron, and the differential continuum oscillator strength df_{p0}/dE_p, with E_p as the energy of the ejected electron from the initial 0 state to the final p state. The Coulomb field of an ionic target distorts the wave function of the incident electron throughout the entire path of its motion, whereas a neutral target does so only in its vicinity. Qualitatively, the charge distribution of the incident electron is attracted towards the target ion, thus increasing the overlap between the charge distributions of the incident and target electrons and producing an enhancement of cross sections. In both the BED and BEB model, the increase in the cross section is accounted for by scaling the Burgess denominator [31,32]. In line with this, we modify siBED [29], by changing the denominator with scaling the Burgess denominator in the Mott part with the inclusion of the charge parameter q. The model, so framed, is henceforth referred to as QIBED. The relativistic ingredients are absent in both the iBED and siBED models, thus making them inapplicable to the relativistic domain. To deal with EII in the relativistic domain, we further modify the QIBED model by infusing in it relativistic corrections. The resulting model is denoted as RQIBED throughout this paper.

The eletron impact ionization of the helium isoelectronic series is one of the most important ion-creation processes from the basic viewpoint. The data for the ionization cross sections for the heliumlike ions form an ideal testing ground next to the hydrogenlike system for a detailed comparison between the experiment and theory. This is due to the fact that the theory is to deal with only two electrons of the target. In this paper we have examined the proposed QIBED and RQIBED models [30] on a wider spectrum of heliumlike species between He and U^{90+}.

To adjudge the performance of the QIBED and RQIBED models, the predictions of these models are compared with those of the siBED model and available experimental data over a wide range of incident energies. To augment the comparative study, we also calculate the cross sections employing RBEB [28], BRY [16], relativistic DM [33] and RBEA [20], and use the results of the distorted wave Born approximation (DWBA) [34,35], Coulomb-Born (CB) approximation without [36] or with exchange (CBX) [37], and relativistic two-potential DWBA (RTPD) referred to as TPDW01 in Ref. [5]. A brief description of the QIBED and RQIBED models of electron impact ionization is given in Sec. II, discussions on the results are provided in Sec. III, and the conclusions are noted in the last section.

II. OUTLINE OF THE MODEL

We denote the Mott and Born parts of the iBED cross section, respectively, by $\sigma_{\text{Mott}}^{\text{iBED}}$ and $\sigma_{\text{Born}}^{\text{iBED}}$. Then the electron impact single ionization cross section in the iBED model of Huo [29] is given by

$$\sigma_{\text{iBED}} = \sigma_{\text{Mott}}^{\text{iBED}} + \sigma_{\text{Born}}^{\text{iBED}}, \tag{1}$$

where

$$\sigma_{\text{Mott}}^{\text{iBED}} = \frac{4\pi N_0}{k_0^2 + k_b^2 + \alpha_0^2}\left[\frac{k_0^2 - \alpha_0^2}{k_0^2\alpha_0^2} - \frac{\ln(k_0^2/\alpha_0^2)}{k_0^2 + \alpha_0^2}\right] \tag{2}$$

and

$$\sigma_{\text{Born}}^{\text{iBED}} = \frac{8\pi}{k_0^2}\int_0^{(k_0^2-\alpha_0^2)/2} (k_p^2 + \alpha_0^2)^5 \frac{df_{p0}}{dE_p} dE_p \times \int_{K_{\min}}^{K_{\max}} \frac{1 + d_1 t + d_2 t}{K[(K+k_p)^2 + \alpha_0^2]^3[(K-k_p)^2 + \alpha_0^2]^3} dK. \tag{3}$$

In the above equations, $\mathbf{K}=\mathbf{k}_0-\mathbf{k}_1$ denotes the momentum transfer in the unit of $\hbar$ with $\mathbf{k}_1$ representing the momentum of the electron after a collision in the same unit. The maximum and minimum values of K are given in Ref. [38]. N_0 is the number of electrons in the orbit considered. Unless otherwise stated, we have used atomic units all through.

In the siBED model of Huo [29], the following approximation is made:

$$\frac{df_{p0}}{dE_p} = \frac{8\alpha_0^3 N_0 k_p}{\pi(k_p^2 + \alpha_0^2)^3}. \tag{4}$$

In parallel with iBED, the siBED cross section in terms of the Mott and Born parts is given [29] by

$$\sigma_{\text{siBED}} = \sigma_{\text{Mott}}^{\text{siBED}} + \sigma_{\text{Born}}^{\text{siBED}}. \tag{5}$$

To facilitate the inclusion of ionic and relativistic corrections, we write the $\sigma_{\text{Mott}}^{\text{siBED}}$ and $\sigma_{\text{Born}}^{\text{siBED}}$ as follows:

$$\sigma_{\text{Mott}}^{\text{siBED}} = SH, \tag{6}$$

$$S = \frac{4\pi N_0}{k_0^2 + k_b^2 + \alpha_0^2}, \tag{7}$$

$$H = \left[\frac{k_0^2 - \alpha_0^2}{k_0^2\alpha_0^2} - \frac{\ln(k_0^2/\alpha_0^2)}{k_0^2 + \alpha_0^2}\right], \tag{8}$$

$$\sigma_{\text{Born}}^{\text{siBED}} = FG, \tag{9}$$

$$F = \frac{64\alpha_0^3 N_0}{k_0^2}, \tag{10}$$

$$G = \int_0^{(k_0^2-\alpha_0^2)/2} k_p(k_p^2 + \alpha_0^2)^2\, dE_p \times \int_{K_{\min}}^{K_{\max}} \frac{1 + d_1 t + d_2 t}{K[(K+k_p)^2 + \alpha_0^2]^3[(K-k_p)^2 + \alpha_0^2]^3} dK \tag{11}$$

and

$$t = \frac{K^4}{[(K+k_p)^2 + \alpha_0^2][(K-k_p)^2 + \alpha_0^2]}. \tag{12}$$

To account for the ionic enhancement of the EII cross section, we modify the denominator of the factor S in Eq. (7)

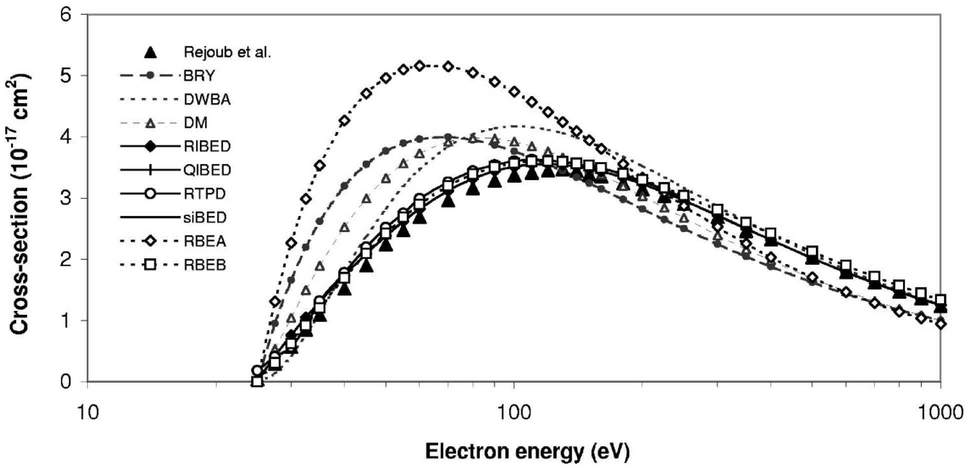

FIG. 1. Electron impact ionization cross section of He as a function of electron energy. Experimental data are from Rejoub *et al.* [42]. The solid curve, solid curve with pluses, and solid curve with solid diamonds denote, respectively, the siBED, QIBED, and RQIBED predictions. The broken curve with solid circles, broken curve with open triangles, broken curve with open diamonds, and broken curve with open squares are, respectively, the calculations from the BRY [16], relativistic DM [33], RBEA [20], and RBEB [28] models. The broken curve is DWBA [34]. The RTPD [5] results are shown as a solid curve with open circles.

occurring in the expression for σ_{Mott} [see Eq. (6)], replacing $k_0^2+k_b^2+\alpha_0^2$ by $k_0^2+(k_b^2+\alpha_0^2)/(q+1)$. The resulting cross section in the QIBED model becomes

$$\sigma_{\text{QIBED}} = \sigma_{\text{Mott}}^{\text{QIBED}} + \sigma_{\text{Born}}^{\text{siBED}}, \tag{13}$$

where

$$\sigma_{\text{Mott}}^{\text{QIBED}} = S'H \tag{14}$$

and

$$S' = \frac{4\pi N_0}{k_0^2 + (k_b^2+\alpha_0^2)/(q+1)}. \tag{15}$$

The expression for σ_{QIBED} does not contain relativistic components in its fold to describe the EII cross sections at the relativistic energies. To augment the expression to the form in the RQIBED model for the relativistic domain, we have made the modifications in the following two stages.

(i) The factor S' in Eq. (15) is replaced by

$$S^R = \frac{4\pi N_0 \alpha^2}{\beta_t^2 + (\beta_b^2+\beta_u^2)/(q+1)}, \tag{16}$$

where

$$\beta_t^2 = 1 - \frac{1}{(1+t')^2} \tag{17}$$

with $t' = k_0^2/(2mc^2)$,

$$\beta_b^2 = 1 - \frac{1}{(1+b')^2} \tag{18}$$

with $b' = k_b^2/(2mc^2)$, and

$$\beta_a^2 = 1 - \frac{1}{(1+a')^2} \tag{19}$$

with $a' = \alpha_0^2/(2mc^2)$. In the above expressions, m is the mass of the electron, c is the velocity of light in free space, and α is the fine structure constant.

(ii) The factor F [see Eq. (10)] for the $\sigma_{\text{Born}}^{\text{siBED}}$ part is replaced by

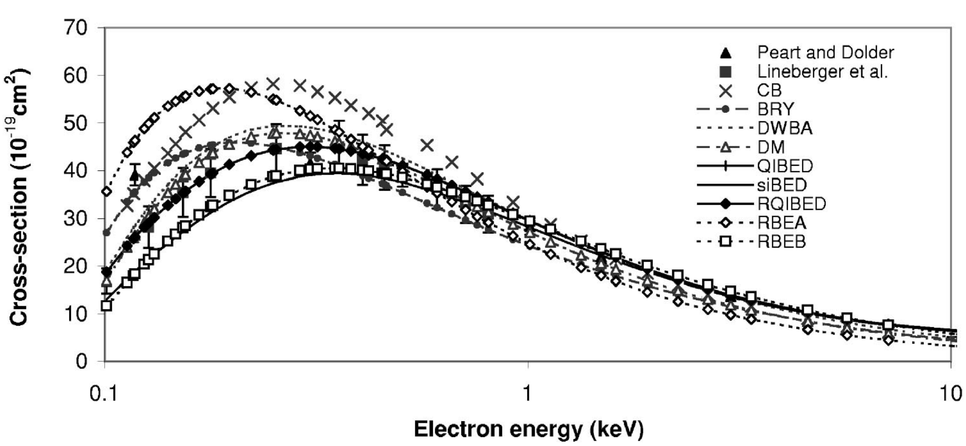

FIG. 2. Same as Fig. 1 for Li^+. Experimental data are from Peart and Dolder [43] and Lineberger *et al.* [44]. The crosses represent the CB predictions [36]. The broken curve is DWBA [34].

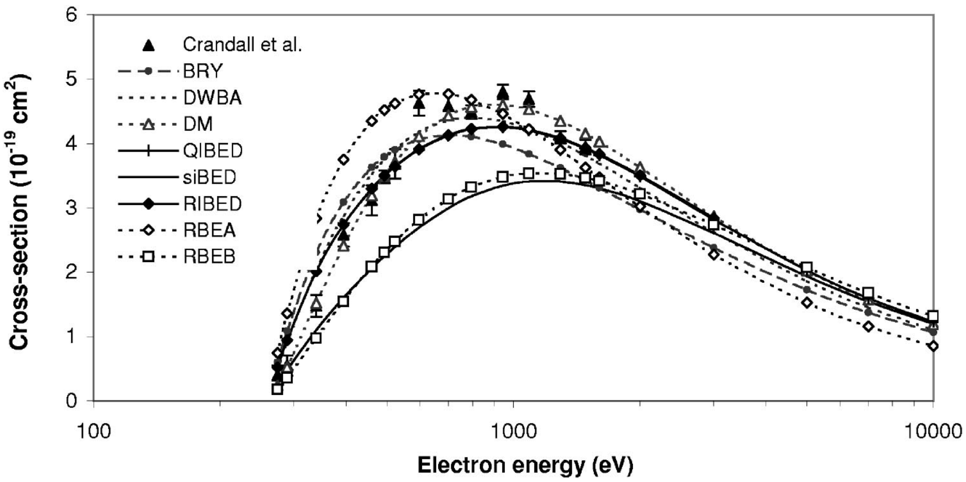

FIG. 3. Same as Fig. 1 for B^{3+}. The data are from Crandall *et al.* [45]. The broken curve is DWBA [34].

$$F^R = \frac{64\beta_a^3 N_0}{\alpha\beta_t^2}. \tag{20}$$

The resulting expression for the EII cross sections in the RQIBED model reduces to

$$\sigma_{\mathrm{RQIBED}} = \sigma_{\mathrm{Mott}}^{\mathrm{RQIBED}} + \sigma_{\mathrm{Born}}^{\mathrm{RQIBED}}, \tag{21}$$

where

$$\sigma_{\mathrm{Mott}}^{\mathrm{RQIBED}} = S^R H \tag{22}$$

and

$$\sigma_{\mathrm{Born}}^{\mathrm{RQIBED}} = F^R G. \tag{23}$$

III. RESULTS AND DISCUSSIONS

The ionization potentials of the targets are calculated using the Dirac-Hartree-Fock code [39]. The radii r_{1s} of the maximum charge density of the orbital required in the DM calculations are obtained from hydrogenlike wave function with the effective charge $Z_{\mathrm{eff}}=Z-5/16$ [40], where Z is the atomic number of the target. The two-dimensional integrations over K and E_p in the siBED, QIBED, and RQIBED models are carried out numerically using the 64-point Gauss-Legendre rule [41]. Following Huo [29], we have made test calculations on the neutral $HeLi^+$ ion. Our observations are the following. By varying d_1 in a step 0.4, the change in the cross section is rather small and smooth, and this is also true for the case with d_2 using the step size of 0.05. Once d_1 is fixed, the other parameter d_2 is determined by an optimal representation of the high-energy part of the cross section. For these two targets, we have found that these parameters have negligible effects on the cross sections at low energies, as expected, but the agreement with the experiment in the high region improves considerably. In the application of the siBED model, the values $d_1=0.0$ and $d_2=0.05$ [29], suggested for neutral molecules, are also found good for He and Li^+ and hence are held fixed for other targets in this study. In Figs. 1–11, the present calculations from the siBED, QIBED, and RQIBED models are compared with the available experimental data: the findings of DWBA [34,35], RTPD [5], and Coulomb Born [36,37] calculations and the present calculations using the RBEB [28], BRY [16], relativistic DM [33], and RBEA [20] models.

A. Ionization of He

The siBED, QIBED, and RQIBED predictions for He are displayed in Fig. 1, along with the experimental cross sec-

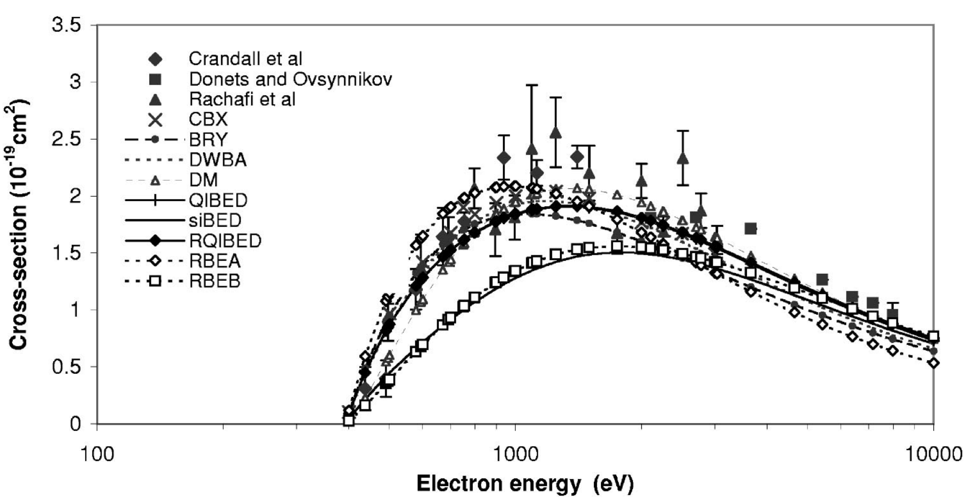

FIG. 4. Same as Fig. 1 for C^{4+}. The data are from Crandall *et al.* [45], Rachafi *et al.* [46], and Donets and Ovsynnikov [47]. The crosses are the CBX calculations from Ref. [37]. The broken curve is DWBA [34].

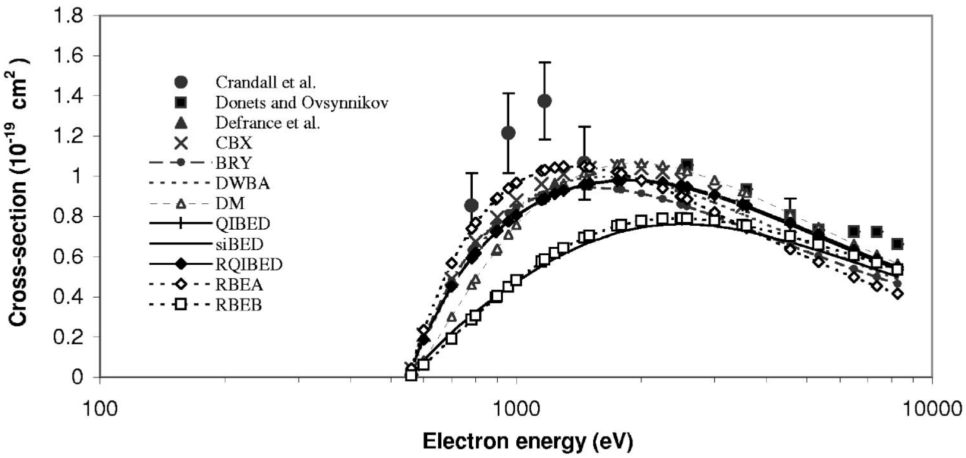

FIG. 5. Same as Fig. 1 for N^{5+}. The data are from Crandall *et al.* [45], Donets and Ovsynnikov [47], and Defrance *et al.* [48]. The crosses are the CBX calculations from Ref. [37]. The broken curve is DWBA [34].

tions [42] and the results of RBEB [28], BRY [16], relativistic DM [33], RBEA [20], DWBA [34], and RTPD [5]. The RBEB, siBED, QIBED, and RQIBED results are almost identical and agree very well with the findings of the experiment and the RTPD calculations. DWBA gives the right pattern of the experimental data with overestimation at the peak position. The DM, BRY, and RBEA calculations fail to describe the experimental data both in magnitude and pattern. The siBED, QIBED, and RQIBED results are almost indistinguishable as there is no ionic correction arising from the neutral target and the relativistic effect in the energy range of the data is negligible.

B. Ionization of Li^{+}

In Fig. 2, we present the calculated cross sections for Li^{+} from siBED, QIBED, and RQIBED, experimental results [43,44], and findings from the RBEB [28], BRY [16], DM [33], and RBEA [20] models, and from the CB [36] and DWBA [34] theories. The large difference between the siBED and QIBED cross sections shows that the contribution from the ionic correction is significant and the siBED is inadequate for an ionic target. RBEB also fails to describe the experimental results at the threshold and peak regions. Within the energy range of the experimental data, the effect stemming from the relativistic correction is negligible to produce a tangible difference between the QIBED and RQIBED results, both showing excellent agreement with the data throughout the entire range of incident energies. DM and DWBA also yield satisfactory fits to the experimental data but the QIBED and RQIBED are distinctly better, particularly in the threshold region. The CB predictions overestimate the experimental cross sections in and around the threshold and peak regions. The results of RBEA largely overestimate the data in the threshold and peak regions and slightly underestimate at the higher energies with its peak position different from the experimental one.

C. Ionization of B^{3+}

The siBED, QIBED, and RQIBED predictions for B^{3+} are depicted, in Fig. 3, along with the experimental cross sections [45] and the RBEB [28], BRY [16], DM [33], RBEA [20], and DWBA [34] results. Both the siBED and RBEB results are alomst similar and underestimate the experimental values at the threshold and peak regions. The QIBED and RQIBED cross sections are almost identical in the studied incident energy range and are seen to produce a good agreement with the experimental data. The difference between the siBED cross sections with those of QIBED or RQIBED is enhanced over than that for the Li^{+} case. The DWBA findings are close to both the experimental and QIBED or RQIBED results. The DM model is definitely doing better than BRY and RBEA. The BRY model generates a fair fit to the data in the threshold region, but drastically underestimates the data in most of the domain including the peak

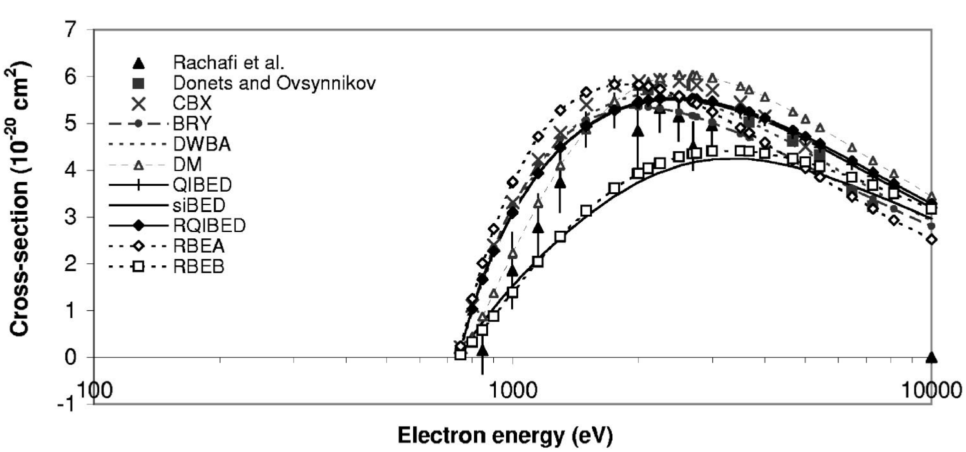

FIG. 6. Same as Fig. 1 for O^{6+}. The data are from Rachafi *et al.* [46] and Donets and Ovsynnikov [47]. The crosses are the CBX calculations from Ref. [37]. The broken curve is DWBA [34].

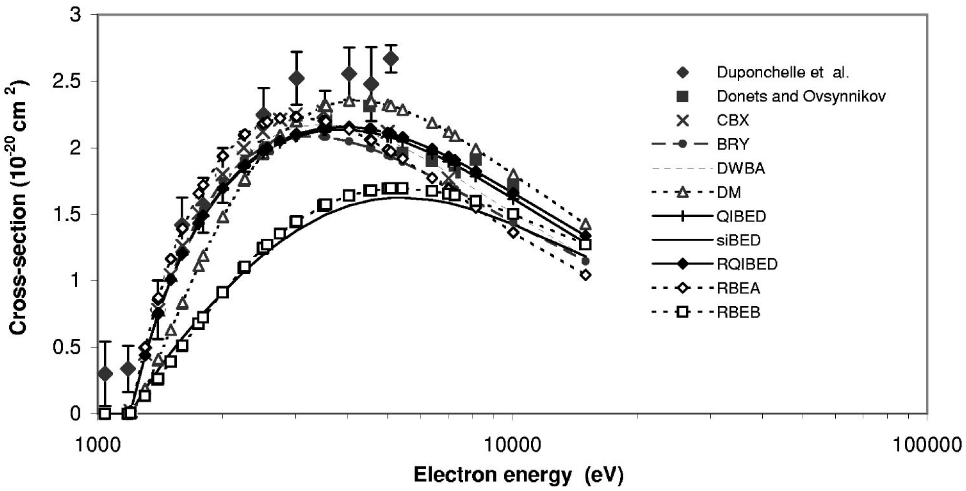

FIG. 7. Same as Fig. 1 for Ne^{8+}. The data are from Donets and Ovsynnikov [47] and Duponchelle *et al.* [49]. The crosses are the CBX calculations from Ref. [37].

region. The RBEA model overestimates the experimental data in the vicinity of the threshold region, but produces reasonable agreement with the data in the remaining region. The discrepancy between the RBEA predictions and the experimental data is reduced from the situation for the previous He and Li^+ targets.

D. Ionization of C^{4+}

Figure 4 compares the predicted cross sections of C^{4+} from siBED, QIBED, RQIBED with the experimental data [45–47], the results from the DWBA [34] and CBX [37] theories, and predictions from the RBEB [28], BRY [16], and DM [33] models. Here again siBED and RBEB cross sections are far from the experimental results in the threshold and peak regions, while both QIBED and RQIBED with their almost identical results produce a good agreement with all three sets of data, marking a clear signature of the substantial contribution from the implemented ionic correction.

While BRY describes the experimental data satisfactorily well in the threshold region, it underestimates the data near and beyond the peak region. The RBEA model produces an excellent agreement with the experimental cross sections up to the peak region but underestimates the data in the region beyond the peak position.

E. Ionization of N^{5+}

In Fig. 5, the siBED, QIBED, and RQIBED results for N^{5+} are compared with the experimental cross sections [45,47,48] and the RBEB [28], BRY [16], DM [33], RBEA [20], DWBA [34], and CBX [37] predictions. The QIBED and RQIBED findings are almost identical, both agree well with one or other of the experimental data sets and are close to the DWBA and CBX results. Here again the siBED results are almost similar to the RBEB predictions and both are far off the experimental cross sections. The large difference persists between the siBED and either of QIBED and RQIBED predictions. The DM calculations definitely underestimates

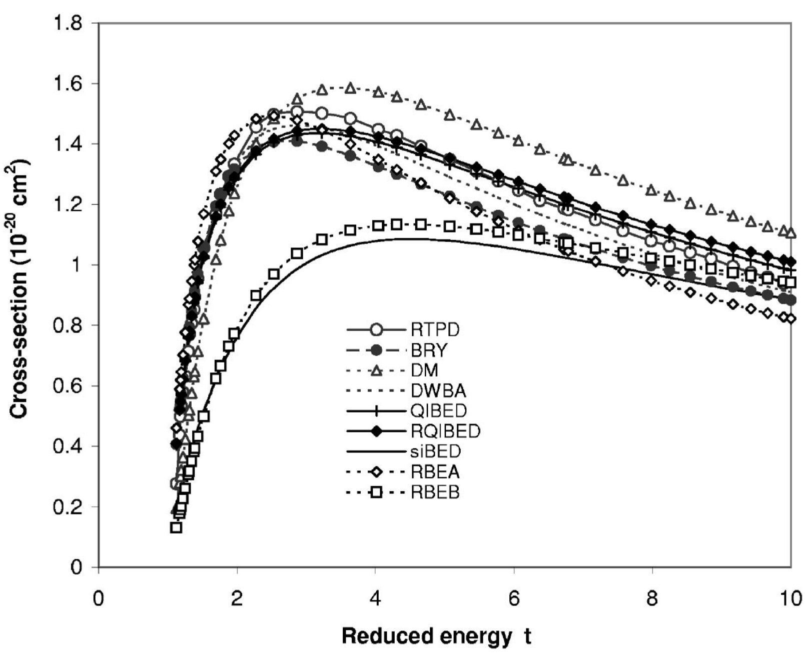

FIG. 8. Electron impact ionization cross section of Na^{9+} as a function of reduced energy t. The curves are the same as in Fig. 1.

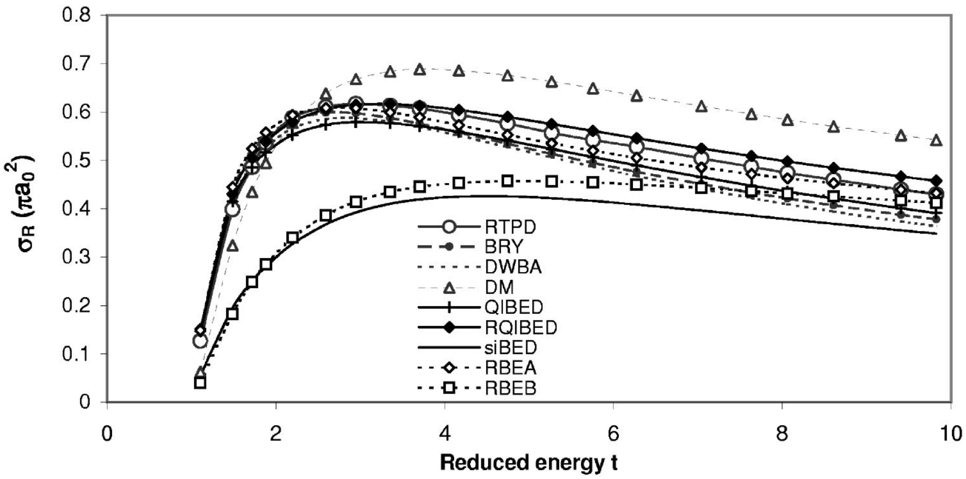

FIG. 9. Reduced cross section of electron impact ionization for Fe^{24+} as a function reduced energy t. The curves are same as in Fig. 1.

in the threshold region but produce excellent agreement with all the experimental data near and beyond the peak region. The BRY calculations perform poorly with the experimental data except at the threshold region. The RBEA results show a close agreement with the experimental data up to the peak region but underestimate the data beyond the region.

F. Ionization of O^{6+}

We compare the siBED, QIBED, and RQIBED results for O^{6+}, in Fig. 6, with both the experimental cross sections [46,47] and the theroretical predictions from RBEB [28], BRY [16], DM [33], RBEA [20], DWBA [34], and CBX [37]. Both the RBEB and siBED cross sections are almost alike and underestimate the experimental data. The QIBED and RQIBED calculations continue to be close to each other, produce a fairly good agreement with the experimental, DWBA, and CBX results, and are far different from those of siBED.

The RBEA model overestimates the experimental data approximately up to the cross-section peak. In the peak region and beyond it, the RBEA model produces a fairly good fit to both the data sets. The BRY calculations overestimate up to the peak, but show fairly good agreement near and beyond the peak. On the other hand, the DM model shows good agreement up to the peak region, but overestimates the data beyond the peak.

G. Ionization of Ne^{8+}

The siBED, QIBED, and RQIBED calculations for Ne^{8+}, in Fig. 7, are compared with the experimental data [47,49]; the predictions from the RBEB [28], BRY [16], DM [33], and RBEA [20] models; and the results from DWBA [34] and CBX [37]. The profound difference between the siBED and QIBED/RQIBED cross sections is contributed from the ionic correction, which enhances the predicted cross sections in good agreement with the experimental data. The CBX, DWBA, BRY, DM, and RBEA results are near to one another, the former two calculations being closer to those of QIBED and RQIBED, which are almost similar with the difference showing at the high-energy end. The RBEA results clearly are closer to the experimental data up to about 8 keV and then fall off in magnitude faster than the data at higher energies. RBEB, similar to siBED, produces results far off from the experimental cross sections.

H. Ionization of Na^{9+}

In view of the unavailability of the experimental EII cross sections for Na^{9+}, to the best of our knowledge, we compare the predicted cross sections from the present QIBED and RQIBED models with those from siBED, RBEB [28], BRY [16], DM [33], RBEA [20], DWBA [34], and RTPD [5] in Fig. 8. The siBED results are greatly underestimated except

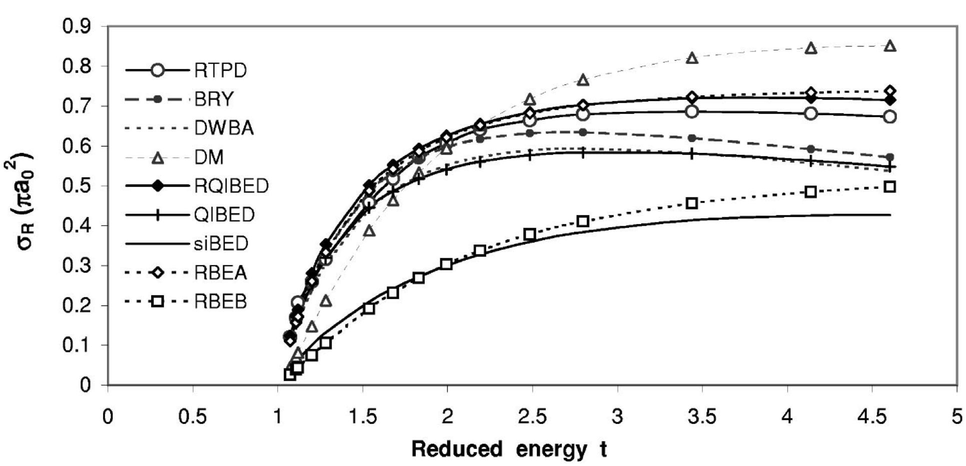

FIG. 10. Same as Fig. 9 for Ag^{45+}.

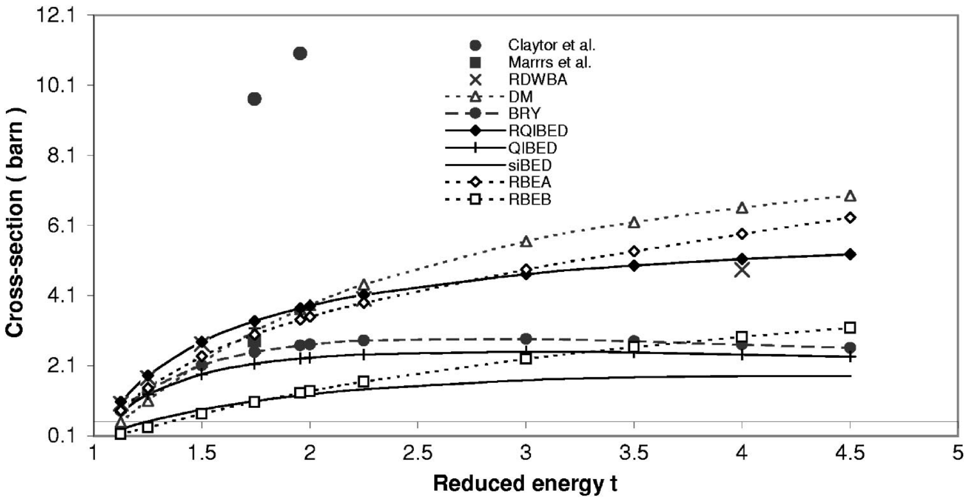

FIG. 11. Electron impact ionization cross section of U^{90+} as a function of reduced energies. Experimental data are from Claytor *et al.* [50] and Marrs *et al.* [51]. The crosses are the RDWBA calculations of Fontes *et al.* [35]. The other curves are the same as in Fig. 1.

at high incident energies from all other predictions, which are close up to and near the peak position. The difference in the QIBED and RQIBED predictions, although small, is now clearly visible at the high-energy end. Both the QIBED and RQIBED results are close to those of DWBA and RTPD. DM gives overestimated cross sections, at the higher energies, compared to the rest of the predictions. The RBEB results, although are almost similar to those of siBED at the threshold and peak regions, quickly catch up the RTPD cross sections at the high-energy end.

I. Ionization of Fe^{24+}

The experimental EII cross sections of the Fe^{24+} ion are also not available to the best of our knowledge. We compare, in Fig. 9, the reduced cross sections (defined by $\sigma_R = \sigma I_{nl}^2 / I_{\mathrm{He}}^2$ with I_{He} as the ionization potential for He), calculated in the present work using the siBED, QIBED, RQIBED, RBEB, BRY, DM, RBEA models with those the DWBA [34] and RTPD calculations [5].

As seen in Fig. 9, the RQIBED curve, which is clearly different from the QIBED one due to the appreciable relativistic effects, is in good agreement with the quantum-mechanical RTPD calculations. RBEA also compares very well with RTPD. Although the DM and DWBA predictions are close to those of RTPD near the threshold region, the disagreement between the former two and the latter begins to appear beyond the peak region and becomes pronounced at higher energies. The siBED results are very different and greatly underestimated compared to the other predictions in the incident energy range considered, except the RBEB findings. The difference between the RBEB and siBED stems from the relativistic effects.

J. Ionization of Ag^{45+}

To the best of our knowledge, the experimental EII cross sections of Ag^{45+} are also not available. The motivation of using a high Z target such as Ag^{45+} is vindicated by the large difference in the QIBED and RQIBED results due to a substantial contribution from the relativistic correction infused in the latter, which predicts cross sections close to those of RTPD. The RBEA results are closer to the RTPD predictions. Both RQIBED and RBEA with relativistic ingredients in their structure are seen to agree much better with RTPD than DWBA. The relativistic DM [33] produces cross sections having large discrepancies with the RTPD results. The remarkable differences amongst the siBED, QIBED, and RQIBED results reflect the substantial size of both the ionic and relativistic effects, and justify the correction factors incorporated in the RQIBED model. The RBEB calculations, although are far from the quantal results at the threshold and peak regions, sharply rise to the RTPD cross sections at the relativistic energies.

K. Ionization of U^{90+}

The siBED, QIBED, and RQIBED predictions for U^{90+} are compared, in Fig. 11, with the experimental data of Claytor *et al.* [50] (at 198 and 222 keV) and Marrs *et al.* [51] (at 198 keV); the present calculations from the nonrelativistic BRY [16], relativistic RBEB [28], DM [33], and RBEA [20] models; and the relativistic DWBA (RDWBA) calculations of Ref. [35]. As seen from the figure, the data of Refs. [50,51] seem to have different normalizations. In particular, at 198 keV ($t = 1.744$), the experimental cross section of the former is 9.7 b, which compares very high relative to the value 2.82 ± 0.35 b of Ref. [51] and 2.88 b, the result estimated by Moore and Reed [52] from the cross section for U^{91+}. The experimental value of Ref. [51] is in close conformity with the sophisticated RDWBA results, the findings from the proposed QIBED, and RQIBED models and the RBEA and DM calculations. The nonrelativistic siBED, QIBED, and BRY calculations as well as the relativistic RBEB predictions are far away from the either sets of experimental data and the RDWBA results. The siBED and RBEB cross sections, which greatly underestimate the experimental cross section of Ref. [51] even at the 198 keV incident energy, underscores the inadequacy of both the siBED and RBEB models for the charged ionic targets and the need for the ionic and relativistic corrections infused in its structure.

IV. CONCLUSIONS

The siBED model, which yields an encouraging description of the EII cross sections on molecules [29], has been found to be excellent as well for a neutral atomic target such as He. The use of $d_1=0.0$ and $d_2=0.05$ for the two parameters in Eq. (11), obtained for the molecules in Ref. [29], seems valid for He. However siBED, similar to the RBEB [28] model, is found to be inadequate for a wide range of ionic targets considered herein. Even in the nonrelativistic region, the siBED model underestimates the experimental cross sections in both the threshold and peak regions, as RBEB does. The discrepancies between the experimental data and the siBED predictions can be greatly mitigated by introducing the ionic correction to the Mott part in the structure of siBED, resulting in the QIBED model. The large differences in the QIBED and the relativistic RDWBA calculations [35] for the U^{90+} target (Fig. 11) underscore the need for relativistic correction in QIBED. In the relativistic domain, it is essential that both the Mott and Born parts of the QIBED model incorporate the relativistic corrections, leading to the proposed RQIBED model. Both QIBED and RQIBED produce almost identical cross sections at nonrelativistic energies. The proposed RQIBED model, with the same values for d_1 and d_2 for all the studied two-electron targets, generates cross sections close to the relativistic RTPD [5] (Figs. 1,8–10), CBX [37] (Figs. 4–7), and relativistic DWBA [35] (Fig. 11) calculations and at the same time shows the best overall agreements with the experimental results amongst the analytical relativistic models, namely, DM, RBEB, and RBEA. considered herein. The RQIBED model with the same two parameters of Ref. [29] produces very encouraging results for all ionic targets. It can be a promising tool for easy and quick generations of the EII cross sections due to its accurate and speedy predictive power.

ACKNOWLEDGMENT

The authors wish to thank Professor F. Bary Malik, Southern Illinois University, Carbondale, USA for fruitful discussion. B.C.S. thanks Professor Andris T. Stelbovics, Murdoch University, Western Australia for fruitful discussions.

[1] S. M. Younger, Phys. Rev. A **26**, 3177 (1982).
[2] I. Bray and A. T. Stelbovics, Phys. Rev. Lett. **69**, 53 (1992).
[3] I. Bray and A. T. Stelbovics, Phys. Rev. Lett. **70**, 746 (1993).
[4] I. Bray, J. Phys. B **28**, L247 (1995).
[5] T.-Y. Kuo and K.-N. Huang, Phys. Rev. A **64**, 032710 (1995).
[6] K. Bartschat, E. T. Hudson, M. P. Scott, P. G. Buke, and V. M. Burke, J. Phys. B **29**, 115 (1996).
[7] K. Bartschat, E. T. Hudson, M. P. Scott, P. G. Buke, and V. M. Burke, Phys. Rev. A **54**, R998 (1996).
[8] K. Laghdas, R. H.G. Reid, C. J. Joachain, and P. G. Burke, J. Phys. B **32**, 1439 (1999).
[9] D. M. Mitnik, M. S. Pindzola, D. C. Griffin, and N. R. Badnell, J. Phys. B **32**, L479 (1999).
[10] M. P. Scott, H. Teng, and P. G. Burke, J. Phys. B **33**, L63 (2000).
[11] A. Riahi, K. Laghdas, R. H. G. Reidf, S. Rachafi, C. J. Joachain, and P. Defrance, J. Phys. B **34**, 175 (2001).
[12] S. M. Younger and T. D. Märk, in *Electron Impact Ionization*, edited by T. D. Märk and G. H. Dunn (Springer-Verlag, Berlin, 1985), p. 24.
[13] D. L. Moores and K. J. Reed, Adv. At., Mol., Opt. Phys. **34**, 301 (1994).
[14] H. Deutsch, K. Becker, S. Matt, and T. D. Märk, Int. J. Mass. Spectrom. **197**, 37 (2000).
[15] W. Lotz, Z. Phys. **232**, 101 (1970).
[16] V. A. Bernshtam, Y. V. Ralchenko, and Y. Maron, J. Phys. B **33**, 5025 (2000).
[17] M. Gryzinski, Phys. Rev. **138**, 336 (1965).
[18] L. Vriens, Proc. Phys. Soc. London **89**, 13 (1966).
[19] M. A. Uddin, M. N. A. Abdullah, M. S. Mahbub, and A. K. Basak, Phys. Scr. **68**, 192 (2003).
[20] M. A. Uddin, A. K. Basak, and B. C. Saha, Int. J. Quantum Chem. **100**, 184 (2004).
[21] H. Deutsch and T. D. Märk, Int. J. Mass Spectrom. Ion Processes **79**, R1 (1987).
[22] Y.-K. Kim and M. E. Rudd, Phys. Rev. A **50**, 3954 (1994).
[23] W. Hwang, Y.-K. Kim, and M. E. Rudd, J. Chem. Phys. **104**, 2956 (1996).
[24] Y.-K. Kim, W. Hwang, N. M. Weinberger, M. A. Ali, and M. E. Rudd, J. Chem. Phys. **106**, 1026 (1997).
[25] M. A. Ali, Y.-K. Kim, W. Hwang, N. M. Weinberger, and M. E. Rudd, J. Chem. Phys. **106**, 9602 (1997).
[26] H. Nishimura, W. M. Huo, M. A. Ali, and Y.-K. Kim, J. Chem. Phys. **110**, 3811 (1999).
[27] W. M. Huo and Y.-K. Kim, Chem. Phys. Lett. **319**, 576 (2000).
[28] Y.-K. Kim, P. Santos, and F. Parente, Phys. Rev. A **62**, 052710 (2000).
[29] W. M. Huo, Phys. Rev. A **64**, 042719 (2001).
[30] M. A. Uddin *et al.* (unpublished).
[31] A. Burgess, in *Atomic Collision Processes*, edited by M. R. C. McDowell (North-Holland, Amsterdam, 1963), p. 237.
[32] A. Burgess, Adv. At. Mol. Phys. **4**, 109 (1968).
[33] H. Deutsch, K. Becker, and T. D. Märk, Int. J. Mass Spectrom. Ion Processes **151**, 207 (1995).
[34] S. M. Younger, J. Quant. Spectrosc. Radiat. Transf. **26**, 329 (1981).
[35] C. J. Fontes, D. H. Sampson, and H. L. Zhang, Phys. Rev. A **59**, 1329 (1999).
[36] D. L. Moores and H. Nussbaumer, J. Phys. B **3**, 161 (1970).
[37] H. Jacubowicz and D. L. Moores, J. Phys. B **14**, 3733 (1981).
[38] M. Inokuti, Rev. Mod. Phys. **43**, 297 (1971).
[39] M. Y. Amusia and L. V. Chernysheva, *Computations of Atomic Processes* (Institute of Physics Publishing, Bristol, 1997).
[40] M. F. Gadi, P. Defrance, A. Makhaute, and M. H. Cherkani, Phys. Scr. **63**, 462 (2001).
[41] F. Scheid, *Numerical Analysis, Schaums Outline Series* (McGraw-Hill, Singapore, 1988).
[42] R. Rejoub, B. G. Lindsay, and R. F. Stebbings, Phys. Rev. A **65**, 042713 (2002).
[43] B. Peart and K. T. Dolder, J. Phys. B **1**, 872 (1968).
[44] W. C. Lineberger, J. W. Hooper, and E. W. McDaniel, Phys.

Rev. **141**, 151 (1966).
[45] D. H. Crandall, R. A. Phaneuf, B. E. Hasselquist, and D. C. Gregory, J. Phys. B **12**, L249 (1979).
[46] S. Rachafi *et al.*, Phys. Scr. **28**, 12 (1989).
[47] E. D. Donets and V. P. Ovsyannikov, Sov. Phys. JETP **53**, 466 (1981).
[48] P. Defrance *et al.*, Nucl. Instrum. Methods Phys. Res. B **9**, 400 (1985).
[49] M. Duponchelle, M. Khoulid, E. M. Onalim, H. Zhany, and P. J. Defrance, J. Phys. B **30**, 729 (1997).
[50] N. Claytor *et al.*, Phys. Rev. Lett. **61**, 2081 (1988).
[51] R. E. Marrs, S. R. Elliot, and D. A. Knapp, Phys. Rev. Lett. **72**, 4082 (1994).
[52] D. L. Moores and K. J. Reed, Phys. Rev. A **51**, R9 (1995).